Synthesis Of Sm³⁺ Substituted Cobalt Ferrite Nanomaterial Using Facile Sol-Gel Technique And Studying Its Effect On Structural And Magnetic Properties Of Cofe_{2-X} Sm_xo₄

Khushboo Kumari^a, Kumar Raj Chittaranjan Singh^b, Sudhir Kumar^c, Raj Kumar Gupta^{d*}, Harendra Kumar Satyapal^e

^{a,c,d,e}Dept. of Physics, Sardar Vallabhbhai Patel College, Bhabhua, Bihar, India ^bNarayan Mahavidyalaya, Gorea Kothi, Siwan, Jai Prakash University, Chhapra, Bihar, India

*Corresponding Author: Dr Raj Kumar Gupta, Senior, Assistant Professor, Head of the Physics Department, Sardar Vallabhbhai Patel College, Bhabhua, Bihar, India. Email I'd; rajkgsw66@gmail.com

In this research paper Samarium-substituted cobalt ferrites $CoFe_{2-x}$ Sm_x O_4 (with x=0, 0.10, 0.20, 0.30) was synthesized using sol-gel method. The structural characterizations of all the prepared samples were done using XRD and FTIR. These studies confirmed the formation of single-phase spinel symmetry in all the compositions with Fd3m space group. The increase in the value of lattice parameter with increase in Sm^{3+} concentration was observed. The Williamson-Hall analysis is used for estimating the average crystallite size and lattice strain induced due to the substitution of Sm^{3+} at Fe^{3+} site. The crystallite size is observed to increase with the concentration of samarium. The surface morphology of samples was determined using SEM. For finding out magnetic parameters like magnetization (M_s) , anisotropy field (B_1) , and magneto crystalline anisotropy (k_1) we used the "Law of Approach to Saturation. Due to the incorporation of Sm^{3+} ions, saturation magnetization (M_s) decreased from 47.3 to 29.2 emu/g and retentivity decreased from 18.5 to 10.1 emu/g. Moreover, as the composition of Sm^{3+} ions increases, Coercivity (Hc) decreases noticeably from 1347 to 932 Gauss. Thus the substitution of samarium strongly influences the magnetic characteristics of cobalt ferrite nanomaterial, and this property can be tailored for its multifunctional applications.

Keywords: Spinel ferrite; Coercivity; Lattice Strain, Ferrimagnetic; Magnetization.

1. Introduction

 $CoFe_2O_4$ with general formula AB_2O_4 has mixed spinel structure denoted by the symbols $[Co_x^{2+}Fe_{1-x}^{3+}]$ $[Co_{1-x}^{2+}Fe_{1+x}^{3+}]$ O_4 and categorized into Fd3m space group [1]. The multiple application of cobalt ferrite such as in recording media, as gas sensors, as magnetic fluids etc. has attracted researches in recent years [2]. The magnetic characteristics like high magnetization and anisotropy possessed by pure $CoFe_2O_4$ and substituted $CoFe_2O_4$ is very interesting. The reported curie temperature of $CoFe_2O_4$ (CFO) is 723 K. Within the spinel unit cell of CFO, 4 crystallographic hard axes, namely 100 and 111, are aligned across the body diagonals of the CFO lattice, whereas the 6 crystallographic easy axes are aligned to cube

edges of the crystal [3]. A unit cell of CFO has 32 octahedral and 64 tetrahedral sites, with O²⁻ occupying the remaining sites. Metal cations occupy just 8 tetrahedral and 16 octahedral sites [4]. As such, the huge empty interstitial voids gives an opportunity to dope it with different ions, for achieving desirable characteristics. The substitution of Co²⁺ and Fe³⁺ sites in the CoFe₂O₄ lattice by any metal cation or by any rare earth ions is reported to enhance its structural and magnetic properties. Many researchers have highlighted the fact that the cationic distribution between the tetrahedral(A) and octahedral(B) sites of CFO can fine tune its electrical and magnetic properties. The presence of the Co²⁺ ion on the B site of such spinel ferrite enhances magneto- anisotropy [5]. The other criterion like lattice parameter, crystallite size, bond angle, and bond lengths are also reported to affect physical characteristics of CFO [6]. Few papers suggest that the synthesis methods employed for CFO synthesis can vary the physical properties of CFO as well [7]. The temperature at which the synthesized CFO nanomaterial is annealed has it's confirm influence on lattice parameters. Weiwei et al. studied the effect of calcination temperature on structural property of CFO nanofibres and suggested nucleation process gets affected by heating[8]. Further, K.Satheesh et al. substituted Ag in CFO lattice and studied it's effect on structural and magnetic properties of CFO[9]. B.R.Kumar et al. explored the thermoelectric properties of Gd substituted CFO[10]. S.Supriya et al. studied the electrical properties of Mn substituted Cobalt ferrite. In this paper AC and DC transport properties were correlated with Mn doping in CFO[11]. Jing Jiang et al. studied La doped CFO and found that saturation magnetization decreased with increasing La concentration. However Coercivity was observed to increase with increasing La ions in CFO lattice[12]. Dipali et al. substituted Zn in CFO lattice and found that magnetization(Ms) increased upto 0.2 mole Zn concentration, thereafter Ms value decreased[13]. Thus a thorough assessment of the literatures reveals that the cationic substitutions at Fe and Co sites by with different ionic radii can successfully refine the physical characteristics of CoFe₂O₄. Therefore, in this article, we report of the synthesis of pure cobalt ferrite by an economical sol- gel auto combustion route and improvement in structural and magnetic properties of CoFe₂O₄ with Sm³⁺ substitution to justify its utility for various technological applications.

2. Experimental details

2.1. Materials and method

The citrate precursor sol-gel method was used to synthesize CoFe2O4. Pure standard chemicals, such as Co (NO₃)₂, Sm (NO₃)₃, Fe (NO₃)₃ were employed in the synthesis process. Citric acid was used as chelating agents during synthesis. At first all the chemicals were taken in stoichiometric amount as per the molecular formula of cobalt ferrite. Then mixed in deionized water individually. In a single beaker these participating solutions were poured. Next job is to change the solution Ph to 7-8(neutral) using ammonia. Finally, this beaker was kept on magnetic stirrer with hot plate temperature 80°C till the time we get a thick jelly-like product. Generally it takes 4 to 5 hours to get thickened. Finally we keep this thick jelly product in a hot air oven for 30 min at temperature 200°C. The result is a voluminous powder product, which is grinded and sent for annealing purpose. The powdered samples were then placed in separate alumina crucibles and heated to 550 °C for two hours at a rate of 4 °C/min

in annealing furnace. These produced nanoparticles were then provided for various characterizations.

2.2. Characterizations

The X-ray diffraction data were obtained at a wavelength (λ =1.5406 Å) using the Bruker D8 advance X-ray Diffractometer. Hysteresis loop (M-H) loops were calculated using Vibrating Sample Magnetometer (capacity 5 Tesla). The morphology study was carried out using SEM (Carl Zeiss). The functional groups present in samples and bond lengths were found using FTIR, (Perkin Elmer). For FTIR analysis, the powdered samples were first palletized into disc shape of diameter 10 mm and thickness 2 mm. For XRD, VSM and SEM testing's, samples were in powdered form.

3. Results and discussion

3.1. X-ray diffraction analysis

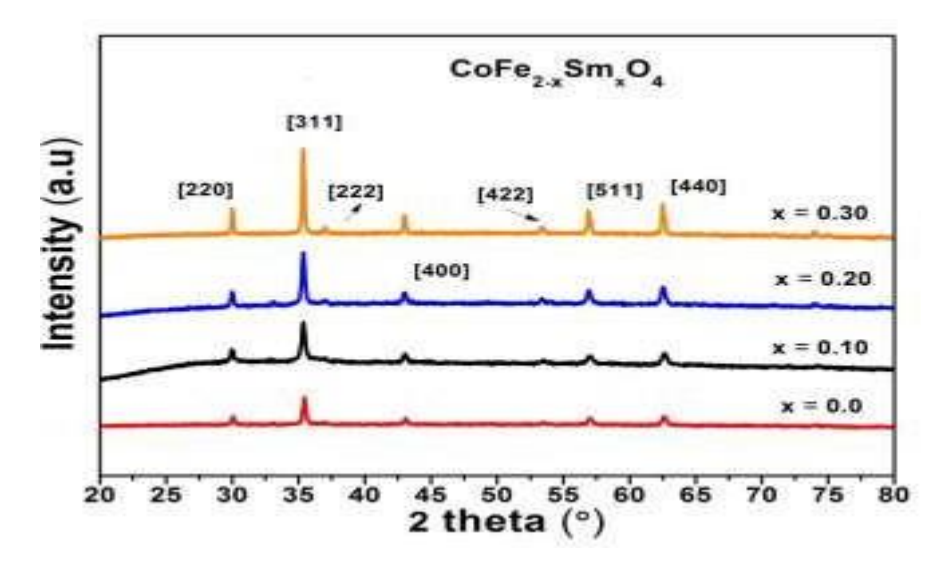


Fig. 1. XRD pattern of $CoFe_{2-x}Sm_xO_4$ for (x = 0.10 to 0.30)

Fig. 1 shows the X ray diffraction intensity peaks for all the samples prepared of $CoFe_{2x}Sm_xO_4$ for (x= 0.10 to 0.30). If reflects all the signature planes of cobalt ferrite indexed Fd3m space group [14]. As no extra peaks were present in the XRD patterns, we can say that pure phase synthesis. The most intense peak [311] is seen to get intensified with the increasing concentration of samarium in the cobalt ferrite lattice. In fact we can see monotonous increase in the intensity of other planes [220], [511], [440] as well with respect to samarium concentration.

The Williamson-Hall (W-H) plot is utilized to find crystallites size and lattice strains in cobalt ferrite lattice (Fig. 3). The W-H equation is given by [15]

In the above equation (1), θ is Bragg's diffraction angle and λ is the wavelength of x-ray used. D is the crystallite size, and β is FWHM. The word (4Sin θ) is the strain effect, and the intercept (K λ /D) on y axis is equated with (β cos θ) value to reveal the sizes of the crystallites in the samples. Fig. 2 displays the W-H plots for the sample CoFe_{2-x}Sm_xO₄ for (x=0.30). Data points from the XRD graph is fitted linearly. The value of lattice strain is directly the slope of the straight line. Table 1 lists all these parameters.

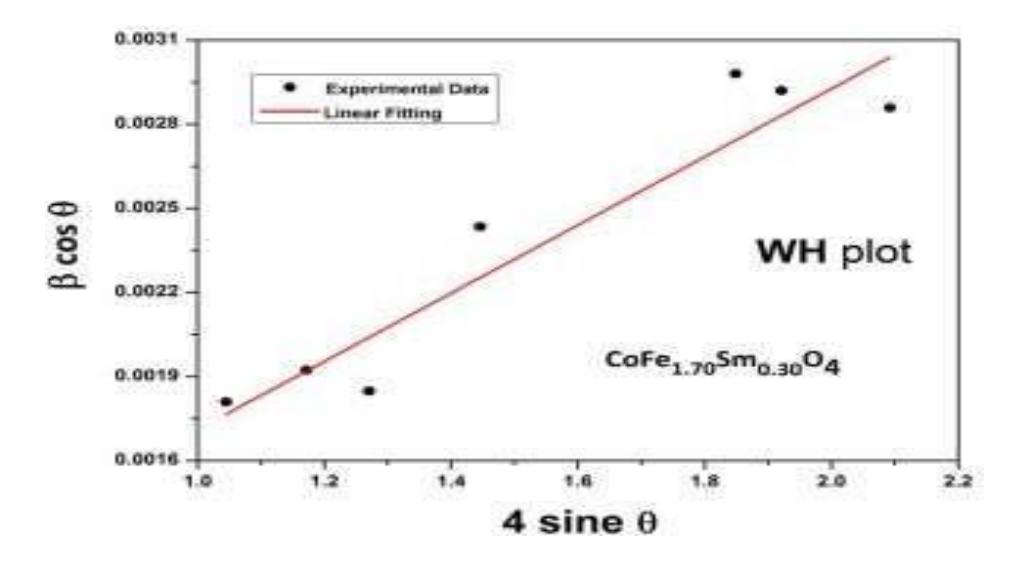


Fig. 2. W-H plots to calculate crystallites size and lattice strain in CoFe_{1.70} Sm_{0.30}O₄

We calculated lattice constants using equation (2), in which significant planes [311], [220], [440], [400] and [511] were used.

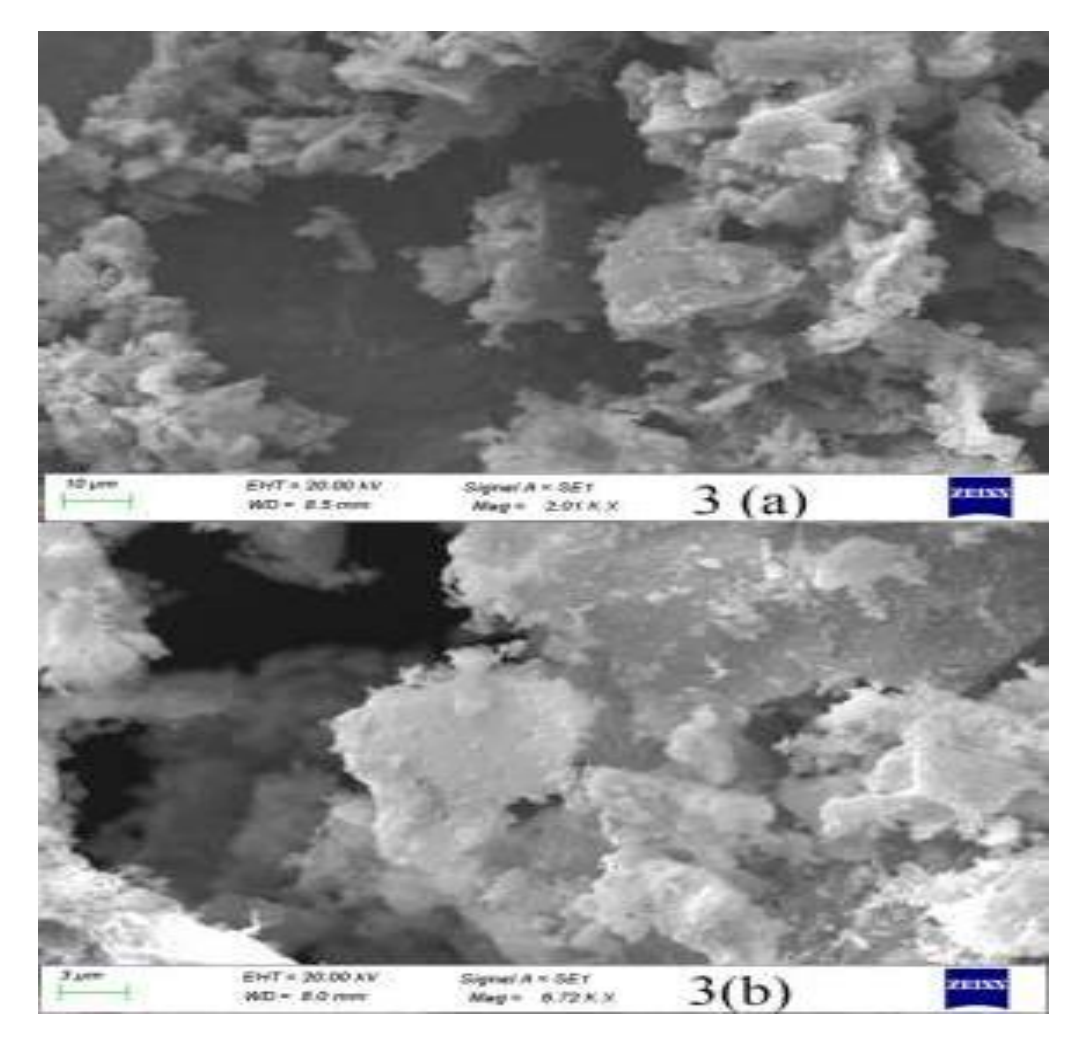
(2)

It is obvious that the lattice strain rises monotonically with the Sm concentration up to x=0.20. For further increase in Sm composition, lattice strain tends to decrease, suggesting that optimized substitution at Fe site to be x=0.20. One of the reason can be attributed to the fact that the ionic radii of Sm ions is 0.964 Å and Fe ions has ionic radii of 0.645 Å only. It is evident that the lattice constant (a) and, therefore, the lattice volume have increased monotonically up to Sm= 0.20 mole. It was noticed that crystallite size increased as Sm concentration rises. This might be as a result of the agglomerations created by annealing, as shown by the SEM morphological analysis covered in section 3.2.

Table 1. Structural details of $CoFe_{2-x}Sm_xO_4$ for (x= 0.10 to 0.30)

CoFe ₂ -	Crystallite size (Williamson- Hall) nm (± Error)	Strain ×10 ⁻³	Crystal structure details		
$_{x}Sm_{x}O_{4}$			a=b		
			=c(Å)	cell volume(ų)	
X=0.0	48.8 (±1)	1.42	8.379	588.269	
X=0.10	57.7 (±1)	1.94	8.405	593.763	
X=0.20	$73.4 (\pm 1)$	2.43	8.417	596.309	
X=0.30	$85.7 (\pm 1)$	1.84	8.408	594.399	

3.2 SEM analysis



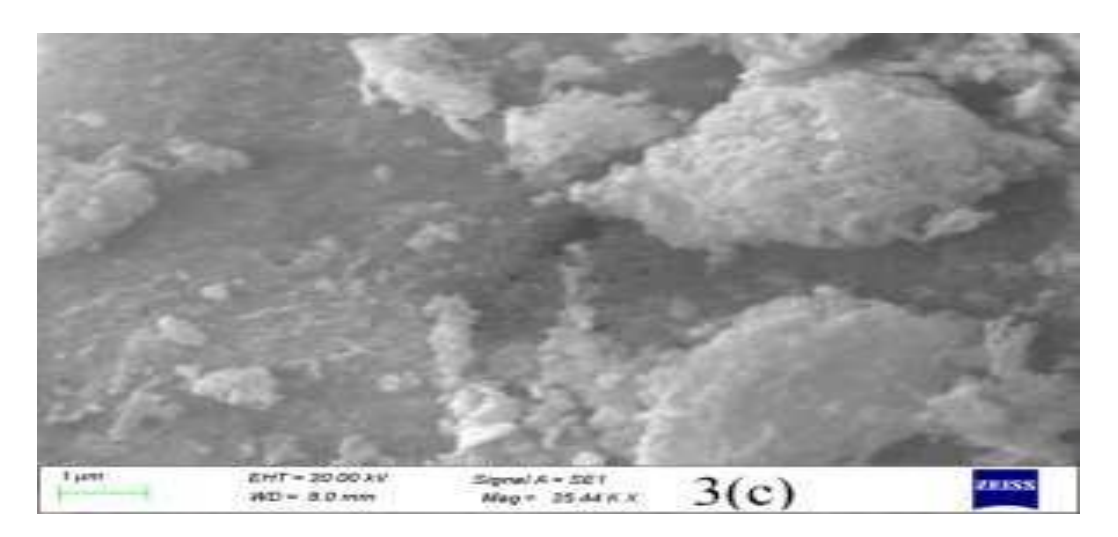


Fig. 3(a-c). SEM micrograph of $CoFe_{2-x}Sm_xO_4$ for (x=0.30) at varied magnifications For morphological study of the samples Fig. 3(a-c) shows the SEM images of $CoFe_{1.70}Sm_{0.30}O_4$ at different magnifications. Particles appear to be uniformly distributed but agglomerated at some areas. When compared to the XRD results, the particle size obtained by SEM is bigger. $CoFe_{2-x}Sm_xO_4$ for (x=0.10 to 0.30) have average particle sizes of 117.04 nm. Particle size is determined using imageJ software and analyzing concern histograms.

3.3 FTIR analysis

FTIR absorption spectra for $CoFe_{2-x}Sm_xO_4$ (x=0.10 to 0.30), captured in the wavenumber range (400 - 700 cm-1), are shown in Fig. 4. Two significant infrared peaks for spinel ferrites, such as $CoFe_2O_4$, are observed at wavenumbers 439 cm⁻¹ and 602 cm⁻¹, respectively, for bonds occurring at the octahedral sites and tetrahedral sites respectively [16].

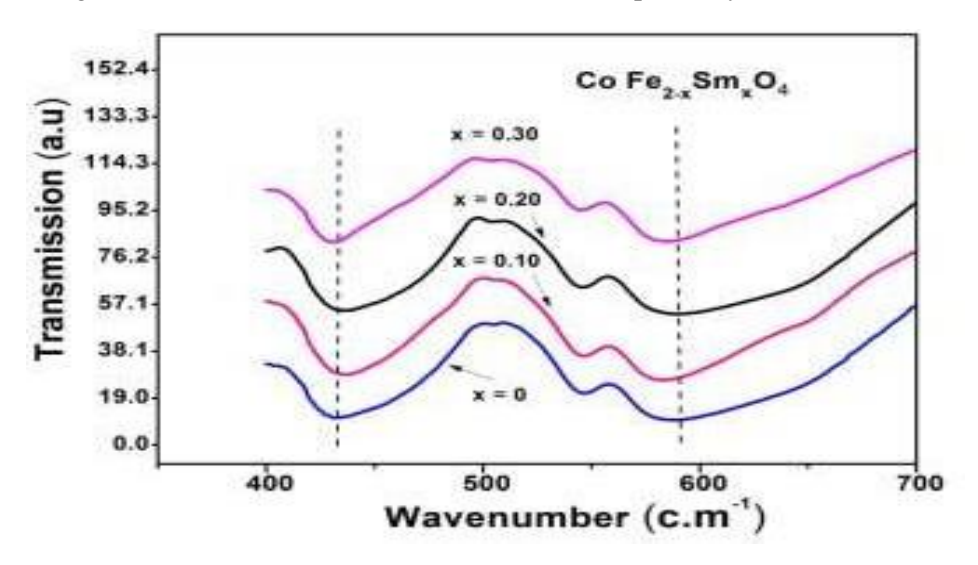


Fig. 4. FTIR spectrum of $CoFe_{2-x}Sm_xO_4$ for (x= 0.10 to 0.30)

For estimating octahedral bond length, the frequency range (422 - 439 cm⁻¹) is employed. The length of the tetrahedral bonds between (Fe-O) and (Co-O) is determined using the frequency limit (590 - 602 cm⁻¹) [17]. Tetrahedral sites have a higher vibrational frequency than octahedral sites because their bonds are longer. The frequency (v) of the vibration with the force constant (K) is used to determine the lengths of the metal-oxygen (M-O) bonds. The frequency of the harmonic oscillation is related as [18]

(3)

Where C denotes the velocity of light. Moreover, force constant (K) is related to bond length (r) as [19]

(4)

As the Sm concentration rises, we can see in Fig. 4 that the absorption peaks gradually move towards a larger wavenumber value. This change may have a likely cause, which could be the stretching of the M-O bonds brought on by induced lattice strain in samples having a Sm³⁺ substitution. Bond lengths at the octahedral sites (12k, 2a, and 4f2) are seen to lengthen due to the structural distortion caused by the big ionic radii of Sm (0.964Å) replacing Fe ions (0.645Å).

3.5 Magnetic Properties

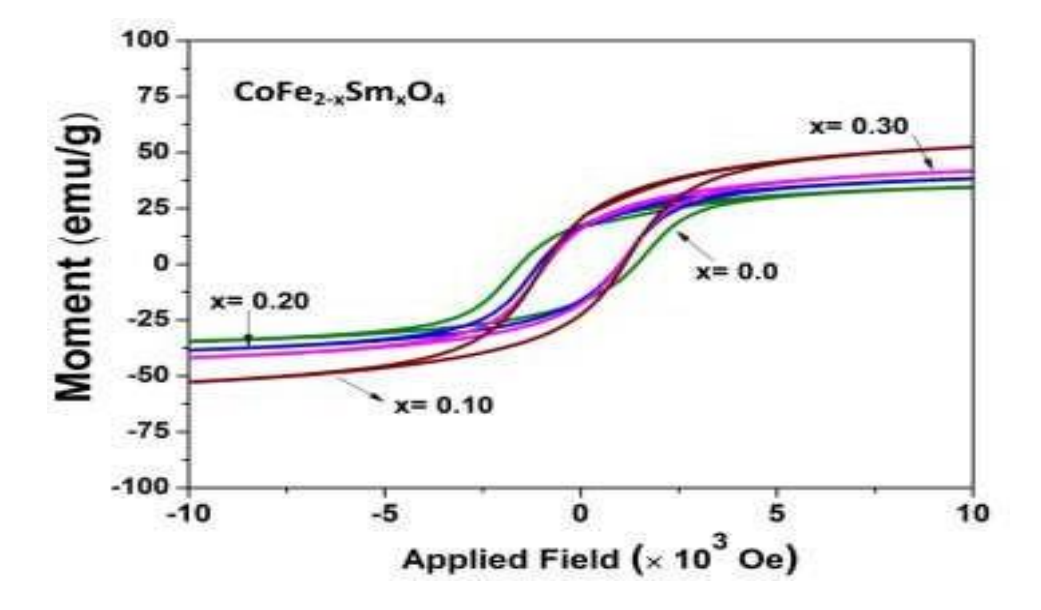


Fig. 5. MH loops at room temperature for $CoFe_{2-x}Sm_xO_4$ for (x = 0.10 to 0.30) hows the magnetic hysteresis (MH) loops of $CoFe_{2-x}Sm_xO_4$ for x = 0.10 to 0.30

Fig. 5 shows the magnetic hysteresis (MH) loops of $CoFe_{2-x}Sm_xO_4$ for x=0.10 to 0.30. The ferrimagnetic behavior and moderate coercivity values are displayed by hysteresis curves. Hysteresis curves seem to reach saturation in the ∓ 1.5 Tesla applied magnetic field. Table 2 lists the computed values for coercivity (H_C), magnetization (M_s), retentivity (M_r), and anisotropy (K₁).

Table 2. Wagnetic parameters details of Core204 samples									
	CoFe ₂₋ _x Sm _x O ₄	Magnetizat ion (Ms) (emu/g)	Retentivity (Mr) (emu/g)	Squarene ss ratio	Coercivit y Hc(Oe)	Anisotropic constant $K_1 \times (10^6 \text{ erg/cm}^3)$			
	x = 0.0	47.3	11.01	0.45	1347	7.25			
	x = 0.10	44.5	18.52	0.40	1017	5.06			
	x = 0.20	37.1	10.15	0.38	996	2.89			
	x = 0.30	29.2	12.08	0.44	932	4.14			

Table 2. Magnetic parameters details of CoFe2O4 samples

With an increase in Sm^{3+} concentration, the remanance and saturation magnetization, M_r and M_s , both decreases monotonically up to x=0.20. As magnetization and the hyperfine field have a linear connection, M_s decreases as the hyperfine field does [20]. The $CoFe_2O_4$ material with a Sm concentration of x=0.10 has the highest coercivity values. It's interesting to observe that coercivity values decreases monotonically as Sm content. One reason for this observation is that, in the applied field ~1.5Tesla, the samples achieved saturation with maximum Sm content of 0.30 moles at Fe^{3+} site. Second reason is the samples' decreased anisotropy as a result of the redistribution of cations brought on by Sm^{3+} replacing Fe ions, causing the coercive field to decrease [21].

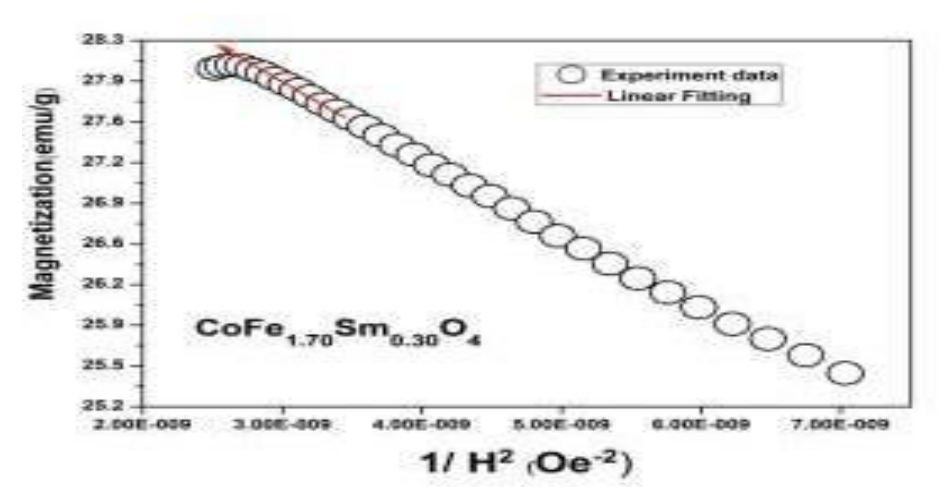


Fig. 6. MH loops at room temperature for $CoFe_{2-x}Sm_xO_4$ for (x = 0.30)

The "Law of Approach to Saturation" is used to calculate key magnetic properties including M_s , the anisotropy constant (K_1) , and anisotropy fields (B). The approach law is provided by [22].

(5) Here (M_s) represents magnetization, A is a material constant, and B is the magneto-crystalline anisotropy field. Ignoring insignificant terms equation (6) reduces as

The anisotropy is expressed as [23]

)]

(6)

Nanotechnology Perceptions 19 No. 3 (2023) 485-494

(7)

The magnetoanisotropy is determined using the relation

(8)

The value of magnetization (M_s) is determined by the intercept on the y-axis of the M versus (1/H²) plot of the experimental data that were linearly fitted (Fig.7). The magneto anisotropy field's value (B_1) is immediately quantified by the slope of this linearly fitted curve. Equations (7) and (8) are then solved to determine the magneto crystalline anisotropy (K_1) value after obtaining the M_s and B_1 values. Table 2 lists all the relevant magnetic parameters. In conclusion, $CoFe_2O_4$ with Sm=0.10 has the highest saturation magnetization and magneto crystalline anisotropy constant. The increase in saturation magnetization is due to the increased magnetic moment, since the magnetic moment bears a linear relationship with the magnetization [20]. Further, M_s decreases from 47.3 to 29.89 emu/g, whereas K_1 is ranging from 7.25×10^6 erg/cm³ to 2.89×10^6 erg/cm³. The observed decrease in anisotropy constants may be due to increased lattice strain. The coercive field is higher for $CoFe_2O_4$ with Sm=0.10, however it is in consistent with the decrease in anisotropic constant. The coercivity of these nanomaterials, which is of the order of 1347 Gauss, suggests that they might be useful in applications involving perpendicular recording medium [23].

4. Conclusions

Using a low-cost citrate precursor sol-gel approach, the cobalt ferrite CoFe_{2-x}Sm_xO₄ for (x= 0.10 to 0.30) was effectively created, and it was then control annealed at 550°C for two hours at a rate of 4°C/min. The XRD examination of the samples' verified spinel crystal symmetry with Fd3m space group. The Sm³+ substitution causes an increase in the lattice parameters (a) and lattice volume. With increasing Sm concentration in CoFe₂O₄ lattice, crystallite size decreased but lattice strain increased. Stretch in the metal-oxygen bonding caused by induced lattice strain is justified by the FTIR spectra. The substituted CoFe_{2-x}Sm_xO₄ has the maximum saturation magnetization at (x= 0.20), with an order of 44.5 emu/g. Also the substituted CoFe_{2-x}Sm_xO₄ has a maximum coercivity value of 1017 Gauss for x= 0.10 and this sample has the highest anisotropy field values. One of the causes suggested may be enhanced distortion in Fe-O network with bigger ionic radii of Sm ions (0.964Å) at Fe site. CoFe₂O₄ improved magneto anisotropy values suggests its potential multifunctional uses. The current work provides a window into how lattice strain can fine tune the structural and magnetic properties of Sm³+ substituted cobalt ferrite.

Acknowledgments

The authors are thankful to UGC, India, for availing RGNF Fellowship as financial assistance. The authors are also thankful to the Dept. of Physics, IIT Patna, for providing magnetic characterization facilities.

Conflict of Interest

All the authors confirm that there is no any conflict of interest.

Data Availability

The data that supports the findings of this study are available from the corresponding author upon a reasonable request.

References:

- 1. I. H. Gul and A. Maqsood, "Structural, magnetic and electrical properties of cobalt ferrites prepared by the sol-gel route," Journal of Alloys and Compounds, vol. 465, no. 1-2, pp. 227–231, 2008.
- 2. S.G. Kakade, Y.R. Ma, R.S. Devan, Y.D. Kolekar, and C.V.Ramana, J. Phys. Chem. C 120, 5682 (2016).
- 3. T. Rahman, M. Vargas, and C.V. Ramana, J. Alloys Compds.617, 547 (2014).
- 4. S.V. Mameli, C. Sangregorio, A. Musinu, A. Ardu, C. Innocenti, G. Ennas, T.K. Nguyen, D. Thanh, D. Peddis, D. Niznansky, and C. Cannas, Nanoscale 8, 10124 (2016).
- 5. N. Somaiah, T.V. Jayaraman, P.A. Joy, and D. Das, J.Magn. Magn. Mater. 324, 2286 (2012).
- 6. S. Singhal, T. Namgyal, S. Bansal, and K. Chandra, J. Electromag. Anal. Appl. 2, 376 (2010).
- 7. S.F. Mansour et al. Enhanced magnetic, dielectric properties and photocatalytic activity of doped Mg-Zn ferrite nanoparticles by virtue of Sm³⁺ role J. Alloy. Compd. (2021)
- 8. Weiwei Pan et. al. Materials Letters, Vol 65, (issue 21,22), 3269-3271 (2011)
- 9. M.K.Satheeshkumar, E Ranjith, J. Mag.Mag.Mater., Vol 469, (2019) 691-697.
- 10. Kumar B R, Ravinder D 2002 Electrical Conductivity of Ni-Zn-Gd Ferrites Mater. Lett. 53 441–445.
- 11. S.Supriya, M. Kar, J.Mater.Sci: Mater. Electron(2017).
- 12. J. Jiang, Yan Min Yang, Physica B: Condensed Matter, 399(2), (2007) 105-108
- 13. Deepali D.Andhare et. al. Physica B: Condensed Matter, 583 (412051) 2020.
- 14. M. Mozaffari, S. Manouchehri, M.H. Yousefi, and J. Amighian, J. Magn. Magn. Mater. 322, 383 (2010).
- 15. S.G. Kakade, Y. Ma, R.S. Devan, Y.D. Kolekar, and C.V. Ramana, J. Phys. Chem. C 120, 5682 (2016).
- 16. M.Y. Salunkhe, D.S. Choudhary, S.B. Kondawar, Int. J Metals. (2013).
- 17. M. Azizar Rahman and A.K.M. Akther Hossain, Phys. Scr. 89, 025803 (2014).
- 18. M. A. Khan, M. U. Islam, M. Ishaque, I. Z. Rahman, A. Genson, and S. Hampshire, "Structural and physical properties of Ni–Tb–Fe–O system," Materials Characterization, vol. 60, no. 1, pp. 73–78, 2009
- 19. Y.D. Kolekar, L.J. Sanchez, and C.V. Ramana, J. Appl. Phys. 115, 144106 (2014).
- 20. K.K. Bharathi, L.N. Patr, and C.V. Ramana, J. Mater. Sci. 48, 5063 (2013).
- 21. M. Sharma, S.C. Kashyap, H.C. Gupta, M.C. Dimri, K. Asokan, AIP Adv. (2014).
- 22. H.J. Kown, J.Y. Shin, J.H. Oh, J. Appl. Phys. 75, 6109 (1994).
- 23. A. Hussain, A. Naeem, J. Mater. Sci.: Mater. Electron. 29, 20783–20789 (2018).